Journal of Molecular Catalysis B: Enzymatic 62 (2010) 40–45

Contents lists available at ScienceDirect

Journal of Molecular Catalysis B: Enzymatic

journal homepage: www.elsevier.com/locate/molcatb

Cloning, overexpression, purification, and site-directed mutagenesis of xylitol-2-dehydrogenase from *Candida albicans*

Shiqi Hong, Jinchuan Wu, Hua Zhao*

Industrial Biotechnology Program, Institute of Chemical & Engineering Sciences, Agency for Science, Technology and Research, 1 Pesek Road, Jurong Island, Singapore 627833, Singapore

ARTICLE INFO

Article history:
Received 20 July 2009
Received in revised form 28 August 2009
Accepted 29 August 2009
Available online 6 September 2009

Keywords:
Xylitol-2-dehydrogenase
Cofactor imbalance
Site-directed mutagenesis

ABSTRACT

Xylitol-2-dehydrogenase from *Candida albicans* was cloned and overexpressed in *Escherichia coli*. The purified recombinant XDH has an apparent molecular weight of 40 kDa which belongs to the medium chain alcohol dehydrogenase family and exclusively uses NAD^+ as a cofactor. The recombinant caXDH has a K_M of 8.8 mM and 37.7 μM using the substrate xylitol and NAD^+, respectively, and its catalytic efficiency is 53,200 min^{-1} mM^{-1}. Following site-directed mutagenesis, one of the engineered caXDHs with six mutations at Ser95Cys, Ser98Cys, Tyr101Cys, Asp206Ala, Ile207Arg, and Phe208Ser shifted its cofactor dependence from NAD^+ to $NADP^+$ in which the K_M and k_{cat}/K_M towards $NADP^+$ are 119 μM and 26,200 min^{-1} mM^{-1}, respectively.

1. Introduction

One of the prerequisites for economical production of biofuels from biomass is the efficient utilization of pentose sugars present in the hydrolysate of biomass [1]. Although D-xylose is one of the major pentose sugars in hemicelluloses and the second most abundant sugar in nature, it is not able to be assimilated by native alcohol-fermenting *Saccharomyces cerevisiae* [2]. Significant efforts have been made to engineer *S. cerevisiae* by heterologously introducing D-xylose utilization pathways either from prokaryotes or eukaryotes [3–6].

The common theme in metabolic engineering of *S. cerevisiae* for xylose utilization is the heterologous introduction of D-xylose utilization pathway from fungi which includes xylose reductase (XR) and xylitol-2-dehydrogenase (XDH), together with D-xylulokinase from *Pichia stipitis* (XKS), or overexpression of the endogenous XKS [4,7,8]. Although several yeast strains have been successfully constructed to allow D-xylose to be metabolized for ethanol production, problems such as inefficient xylose utilization and xylitol accumulation remain as major obstacles for efficient ethanol production from xylose. Many studies have unanimously pointed that these problems are caused by inefficient xylose transport and cofactor imbalance as a result of the discrepancy in cofactor preference of XR and XDH, and low activities of introduced XR and XDH [9,10]. Attempts have been made to address the cofactor imbalance either by heterologous introduction of bacterial or fungal xylose isomerase (XI) pathway instead of XR and XDH from *P. stipitis*, or overexpression of the pentose phosphate pathway [11]. However, the resulting *S. cerevisiae* with XI activity has limited xylose fermentation ability.

Another strategy is to shift the cofactor preference of either XR or XDH [12,13]. Both *S. cerevisiae* strains have been reconstructed recently and the performance of the resulting yeasts was improved in terms of xylitol accumulation, xylose uptake rate and ethanol yield when compared to the strain with a cofactor-imbalanced xylose pathway [12,14]. So far, only the engineered XR and XDH from *P. stipitis* with a shifted cofactor dependence are available for construction of a cofactor-balanced xylose pathway in *S. cerevisiae*. It is desirable to have an alternative source of XRs and XDHs with a shift in cofactor dependence and higher activities which may serve as an alternative enzyme source for construction of a recombinant *S. cerevisiae* with a cofactor-balanced xylose pathway. *Candida albicans* is known for its fast and efficient assimilation of pentose [15]. This suggests an active xylose utilization pathway which implies that XR and XDH from this strain might be highly active. Hence, the gene encoding XDH in *C. albicans* was cloned by reverse transcription PCR (RT-PCR) and overexpressed in *Escherichia coli*, followed by site-directed mutagenesis for a shift of the cofactor dependence. With this engineered caXDH, we can proceed with further engineering of xylose utilizing *S. cerevisiae* for a cofactor-balanced xylose pathway.

Abbreviations: RT-PCR, reverse transcription polymerase chain reaction; PAGE, polyacrylamide gel electrophoresis; XDH, xylitol-2-dehydrogenase; XR, D-xylose reductase; IMAC, immobilized metal affinity chromatography.

* Corresponding author. Tel.: +65 67963799; fax: +65 67963133.
E-mail address: zhao_hua@ices.a-star.edu.sg (H. Zhao).

1381-1177/$ – see front matter © 2009 Elsevier B.V. All rights reserved.
doi:10.1016/j.molcatb.2009.08.013

2. Materials and methods

2.1. Strains, plasmids and medium

The gene encoding wild-type XDH, *XYL2*, was isolated from *C. albicans* SC5314 (ATCC number: MYA-2876). *E. coli* DH5a was a host for plasmid transformation, propagation and maintenance. Overexpression of the wild-type and engineered XDH was performed in *E. coli* BL21 (DE3) strain. Plasmid pET21a from Novagen (MERCK, San Diego, CA, USA) was used for overexpression of target enzymes. *E. coli* strains were grown in LB medium supplemented with the appropriate antibiotic. The yeast complex medium YPD which contained 2% yeast extract, 1% peptone, and 2% dextrose was used to culture *C. albicans*.

2.2. Molecular cloning

C. albicans was cultured in YPD medium and induced with xylose for about 3–4 h prior to total RNA isolation. Total RNA was extracted from the *C. albicans* using RNase Plant Mini Kit from Qiagen (Valencia, CA, USA). Qiagen's protocols were followed after initial enzymatic lysis of the freshly harvested cells with lyticase. The first strand of cDNA was synthesized from total RNA using Superscript II reverse transcriptase with an Adapter Primer, 5′-GGC CAC GCG TCG ACT AGT ACT $(T)_{16}$-3′ (Invitrogen, Carlsbad, CA, USA). The product of the RT reaction was used in subsequent PCR reaction.

Using the known XDH of *P. stipitis* (psXDH, GenBank accession number: A16166), a homology search against the genomic DNA sequence of *C. albicans* revealed a hypothetical protein which shares 74% sequence identity with psXDH. Based on the predicted DNA sequence which encodes the hypothetical XDH (GenBank accession number: XP719434), a forward primer (sense 5′-GGA GGA CAT ATG ACA AAC CCT TCT TTA GTG C-3′, *Nde* I site was underlined) and reverse primer (antisense 5′-GG AGG AGA ATT CGC TTC TGG GCC ATC GAT TAA AC-3′, *EcoR* I site was underlined) were designed and used to amplify the cDNA sequence which encodes mature wild-type XDH by RT-PCR.

The PCR reaction was carried out in 50 μl of 1× high fidelity buffer B (New England Biolabs, Ipswich, MA), 5 pmol of each primer, 10 μmol of each dNTP, 1 μl of cDNA templates from the first strand reaction, and 2.5 units of Phusion polymerase with high fidelity for 25 cycles using i-Cycler from BioRad (Hercules, CA, USA). Each cycle consisted of 10 s at 98 °C, 30 s at 58 °C, and 45 s at 72 °C, with a final extension of 5 min. The PCR products were subjected to 1% agarose gel electrophoresis, purified, and digested with *Nde* I and *EcoR* I simultaneously. The resulting DNA was ligated into pET21a using T4 DNA ligase at 16 °C overnight and transformed into competent *E. coli* DH5a cells for amplification, purification and sequencing. The constructed plasmid which carried a C-terminal 6× His tag sequence was designated as pET21a-XDH.

2.3. Site-directed mutagenesis

A previous study on XDH from *P. stipitis* revealed that three amino acid residues (Asp207, Ile208, and Phe209) in the cofactor-binding pocket determined the cofactor dependence of XDH and the introduction of other 3 cysteine residues at position of Ser96, Ser99, and Tyr102 enhanced the thermal stability of psXDH [13]. Since the deduced XDH from *C. albicans* shared high sequence homology with psXDH and those amino acid residues were highly conserved, we predicted that those amino acid residues in XDH of *C. albicans* (Ser95, Ser98, Tyr101, Asp206, Ile207, and Phe208) played similar roles. In addition, Arg residues in the binding pocket were identified to form a positive binding pocket for the 2′-phosphate group of $NADP^+$ [13]. Therefore, site-directed mutagenesis was performed on those amino acid residues by overlap extension PCR (OE-PCR). To create XDH mutants which was designated as C4ARS mutants and contained the six point mutations (Ser95Cys, Ser98Cys, Tyr101Cys, Asp206Ala, Ile207Arg, and Phe208Ser), the overlapped fragments encoding partial gene of caXDH were PCR-amplified with three pairs of oligos (frag1-for, 5′-GGA GGA **CAT ATG** ACA AAC CCT TCT TTA GTG C-3′; frag1-rev, 5′-GTT TCC TGA CTT *GCA* CTC GTC *GCA* GTA TCT *GCA* CGG GAC ACC-3′; frag2-for, 5′-GGT GTC CCG *TGC* AGA TAC *TGC* GAC GAG *TGC* AAG TCA GGA AAC-3′, frag2-rev, 5′-CAA TTT GTT ATC *CGA ACG CGC* GAC GAC CAT AAT G-3′; frag3-for, 5′-ATT ATG GTC GTC *GCG CGT TCG* GAT AAC AAA TTG-3′; and frag3-rev, 5′-GG AGG A**GA ATT C**GC TTC TGG GCC ATC GAT TAA AC-3′, where italicized sequences indicate mutations introduced and underlined sequences denote restriction sites). The resulting fragments were gel-purified, combined together and assembled by primerless PCR. Final amplification of the complete mutated XYL2 gene was performed by OE-PCR with oligo frag1-for and frag3-rev. The DNA bands on the agarose gel with the desired size were excised, purified, digested simultaneously with *Nde* I and *EcoR* I, and cloned into pET21a for overexpression in *E. coli* BL21 (DE3). A similar strategy was applied to create another XDH mutants designated as C4ARSdR with one more mutation at Asn300Arg but with oligos frag2R-rev (5′-5′-CAT TTG CAA TTT *ACG* ATC *CGA ACG CGC* GAC GAC CAT AAT G-3′) and frag3R-for (5′-ATT ATG GTC GTC *GCG CGT TCG* GAT *CGT* AAA TTG CAA ATG-3′), to replace frag2-rev and frag3-for, respectively, during PCR amplification of fragment 2 and 3 by OE-PCR. The point mutations introduced were further confirmed by DNA sequencing.

2.4. Protein overexpression and purification

The constructed plasmid pET21a-XDH was transformed into chemically competent *E. coli* BL21 (DE3) by heat shock. A single colony was randomly picked up from the transformation plate and inoculated into 3-ml LB medium supplemented with 50 μg/ml ampicillin (Amp) for overnight cell culture. The resulting overnight cell culture was inoculated into 300 ml LB with 50 μg/ml Amp, incubated at 37 °C and 260 rpm until the $OD_{600\,nm}$ reached 0.6–0.8. Overexpression of the recombinant proteins was induced by adding IPTG to a final concentration of 0.5 mM at 25 °C for 10 h.

Recombinant cells were harvested by centrifugation at 6371 × *g* and 4 °C for 15 min using Allegra™ 25 Centrifuge from BECKMAN COULTER™ (Fullerton, CA, USA). To disrupt the cells, the cell pellet was resuspended into 20 ml lysis buffer containing 20 mM Tris, 0.5 M NaCl, 100 g/l glycerol and 10 mM imidazole at pH 7.5 with 1 mg/ml lysozyme and deeply frozen in a −80 °C freezer. The thawed mixture was disrupted by sonication using BRANSON Digital Sonifier (Danbury, CT, USA), followed by centrifugation at 12,000 rpm to remove the cell debris. The supernatant was recovered for protein purification.

Purification of the recombinant protein was accomplished by an immobilized metal affinity chromatography (IMAC) using metal chelating column charged with Zn^{2+} with AKTA Purifier from GE Healthcare (Piscataway, NJ, USA). The equilibration buffer contained 20 mM Tris, 0.5 M NaCl, 100 g/l glycerol, and 50 mM imidazole at pH 7.5, whereas the elution was achieved using the same buffer but containing 200 mM imidazole. After the supernatant from the cell pellet was loaded onto the pre-equilibrated IMAC chelating column, the column was flushed extensively with 10 column volume of binding buffer and then eluted with 8 column volume of the elution buffer. Elution was monitored at 280 nm with a UV monitor, and 1-ml fractions were collected. Peak absorbing fractions were pooled and analyzed on SDS-PAGE. After electrophoresis, the gel was stained with Coomassie brilliant blue R-250 (Serva Fine Chemicals, Westbury, NY, USA). The concentration of the purified recombinant protein was quantified by Bradford assay with bovine serum albumin as standard.

2.5. Enzyme activity assay

Xylitol-2-dehydrogenase activity was routinely detected in 50 mM phosphate buffer at pH 7.5 and 25 °C. The enzyme activity of wild-type XDH towards NAD^+ and engineered XDH towards $NADP^+$ were done by measuring NAD(P)H at 340 nm. The enzyme activity was calculated as units (U), with 1 U corresponding to the conversion of 1 μmol of NAD(P)H per min. The initial velocity data were analyzed by nonlinear least-square regression using the GraphPad Prism. Protein concentrations were determined by Bradford assay with bovine serum albumin as a standard. The thermal stability of XDH was determined by heat inactivation of enzymes at various temperatures using the heat block of i-cycler from Bio-Rad (Hercules, CA, USA). Samples were taken after 15 min of heat inactivation and analyzed for residual activity using Cary UV spectrophotometer from VARIAN (Palo Alto, USA).

3. Results

3.1. Cloning of XDH

With the known XDH from *P. stipitis*, a homology search against the genomic DNA sequences of *C. albicans* revealed a hypothetical protein which shares 74% sequence identity with psXDH. Oligos based on the predicted DNA sequence were designed and the complete cDNA which encodes XDH was isolated by RT-PCR and cloned into pET21a. The deduced sequence (Fig. 1) contains 360 amino acids residues which is in agreement with the prediction by Basic Local Alignment Search Tool (BLAST) (http://blast.ncbi.nlm.nih.gov/Blast.cgi). The deduced caXDH has a molecular weight of 38.8 kDa, which suggests that it belongs to the medium chain alcohol dehydrogenase family. In consistent with the known medium chain XDH, three amino acid residues, Cys40, His65 and Glu158, which were supposed to bind Zn^{2+}, were identified. The NAD^+ binding sites were also conserved based on the deduced sequence (Fig. 1).

3.2. Expression and purification of XDH

Overexpression of the recombinant XDH was performed by transforming the pET21a-XDH confirmed by DNA sequencing to *E. coli* BL21 (DE3) strain. Using immobilized metal affinity chromatography (IMAC) with 1-ml chelating column charged with Zn^{2+}, the XDH overexpressed in *E. coli* BL21(DE3) was purified to homogeneity (Fig. 2). The purified XDH appeared as one band at an apparent molecular weight of 38 kDa determined by the denaturing SDS-PAGE. This was in good agreement with the mass based on the deduced sequence (Fig. 2).

The kinetic parameters of the purified wild-type XDH were also determined. The k_{cat} of XDH was 2000 min^{-1} and the apparent K_M towards xylitol was 8.8 mM. Similar to the known XDHs characterized so far, caXDH exclusively requires NAD^+ rather than $NADP^+$ as a cofactor. As indicated in Table 1, the K_M towards NAD^+ is 37.7 μM, while the initial velocity of XDH towards $NADP^+$ was undetectable due to low activity of the enzyme with $NADP^+$. Various substrates were examined for substrate specificity. As expected, the highest activity for the oxidative reaction was obtained with xylitol (Table 2). The catalytic efficiency of XDH towards D-sorbitol and adonitol was 36%, and 20% of that for xylitol, respectively, whilst XDH activities towards D-mannitol and L-arabitol were less than 1%.

3.3. Site-directed mutagenesis

The deduced sequence of caXDH shared high identity with the known psXDH and the amino acid residues at the cofactor-binding

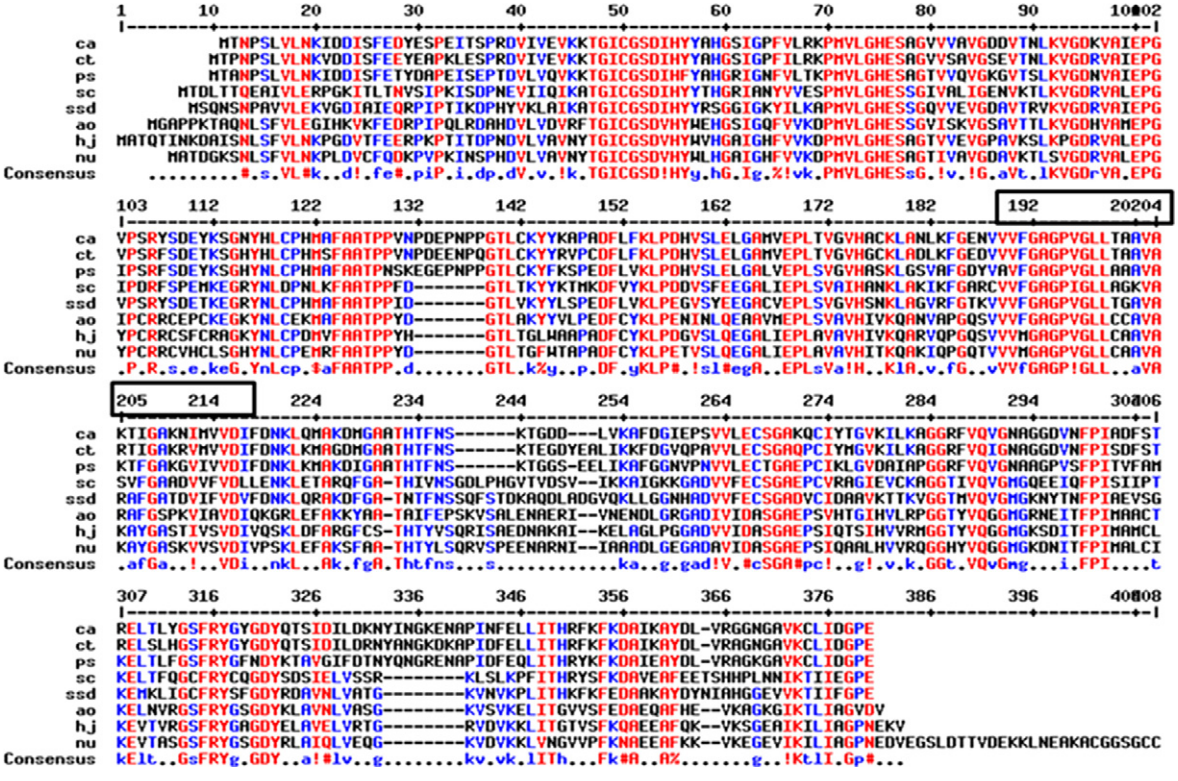

Fig. 1. Sequence alignment of wtXDH of *Candida albicans* with other known XDHs from various microorganisms. The XDHs aligned are from *C. albicans* (ca, GenBank accession no. XP719434), *Candida tropicalis* (cb, GenBank accession no. DQ201637), *Pichia stipitis* (ps, GenBank accession no. A16166), *Saccharomyces cerevisiae* (sc, GenBank accession no. NP013171), *Aspergillus oryzae* (ao, GenBank accession no. BAC75870), *Hypocrea jecorina* (hj, GenBank accession no. AAO42466), and *Neurospora crassa* (nc, hypothetical protein, GenBank accession no. XP964807). The ssd denotes sorbitol dehydrogenase from *S. cerevisiae* with the GenBank accession no. AAA35027. The open square indicates the NAD^+-binding site.

Table 1
Kinetic parameters of wt- and mutant XDH from *Candida albicans* for NAD^+, $NADP^+$, and xylitol.

Enzyme	Specific activity		NAD^+				$NADP^+$			
	NAD^+ (U mg^{-1})	$NADP^+$	K_M (mM)	k_{cat} (min^{-1})	k_{cat}/K_M (min^{-1} mM^{-1})	$K_M^{xylitol}$ (mM)	K_M (mM)	k_{cat} (min^{-1})	k_{cat}/K_M (min^{-1} mM^{-1})	$K_M^{xylitol}$ (mM)
WT	51.7 ± 1.2	1.94 ± 0.15	0.0377 ± 0.0042	2000 ± 50	53200 ± 6060	8.83 ± 1.02	1.69 ± 0.32	75.3 ± 5.7	44.6 ± 9.1	–
C4/ARS	125 ± 9	81.2 ± 1.8	3.25 ± 0.49	4860 ± 340	1500 ± 250	–	0.119 ± 0.010	3120 ± 70	26200 ± 2300	60.9 ± 6.5
C4/ARSdR	150 ± 12	84.3 ± 2.6	5.52 ± 0.08	5790 ± 480	1050 ± 90	–	0.140 ± 0.015	3270 ± 100	23400 ± 2600	85.2 ± 11.2

C4/ARS represents mutants of caXDH carrying six point mutations (Ser95Cys, Ser98Cys, Tyr101Cys, Asp206Ala, Ile207Arg, and Phe208Ser), while C4/ARSdR denotes another mutants of caXDH carrying one more point mutation, Asn300Arg, in addition to six point mutations of C4/ARS.

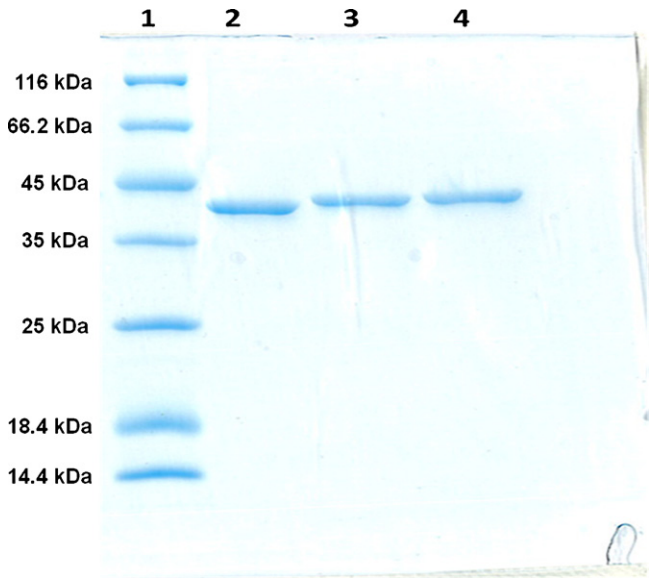

Fig. 2. Analysis of the purified recombinant wtXDH, C4/ARS, and C4/ARSdR on 12% SDS-PAGE. Lane 1, molecular mass marker; lane 2, purified wtXDH; lane 3, purified C4/ARS; lane 4, purified C4/ARSdR.

site were highly conserved. Similar amino acids with psXDH (13) were, therefore, chosen to perform site-directed mutagenesis for a shift of the cofactor preference. Based on the known structure of psXDH, two mutants of XDH, C4/ARS and C4/ARSdR, were created by OE-PCR. C4/ARS contains three point mutations (Asp206Ala, Ile207Arg, and Phe208Ser) in the cofactor-binding pocket and three point mutations (Ser95Cys, Ser98Cys, and Tyr101Cys) to increase the thermostability of wild-type XDH. Additional point mutation, Asn300Arg, was introduced into mutant C4/ARS to create C4/ARSdR mutant. Both mutants were His-tagged at the C-terminal to facilitate subsequent recombinant enzyme purification by IMAC. Unexpectedly, the purified mutants showed a slightly higher molecular weight band than wild-type XDH on denaturing SDS-PAGE.

Using purified recombinant enzymes, kinetic parameters towards both $NADP^+$ and NAD^+ were determined. The catalytic efficiency of both mutants towards $NADP^+$ was 18-fold higher than using NAD^+ as a cofactor, which was comparable with k_{cat}/K_M of 53,200 min^{-1} mM^{-1} towards NAD^+ of the wild-type enzyme. The K_M of C4/ARS and C4/ARSdR towards $NADP^+$ was 119 and 140 μM, respectively, compared with 3250 and 5520 μM with NAD^+ as the cofactor. Additionally, C4/ARS showed better performance than C4/ARSdR in terms of lower K_M and higher catalytic efficiency (k_{cat}/K_M) as indicated in Table 1. Heat inactivation of the enzymes demonstrated that both mutants displayed greater thermal stability than wild-type XDH. When inactivated at 55 °C for 15 min, C4/ARS mutants still retained around 50% of their activities (Fig. 3).

4. Discussion

We have cloned one of the most active XDHs from *C. albicans*. Among the known characterized XDHs, wild-type XDH from *C. albicans* is considered highly active [13,16–19]. Following site-directed mutagenesis, the cofactor preference of XDH from *C. alibicans* was shifted. This mutated XDH can serve as an alternative enzyme source for construction of a cofactor-balanced xylose utilization pathway in *S. cerevisiae*. In addition, the catalytic efficiency of engineered XDH with $NADP^+$ was comparable to the wild-type XDH with NAD^+. To address the cofactor imbalance problem in engineered *S. cerevisiae*, only XDH from *P. stipitis* has been engineered

Table 2
Kinetic parameters of wtXDH from *C. albicans* with other substrates.

C. abicans XDH with indicated substrate	k_{cat} (min^{-1})	K_M (mM)	k_{cat}/K_M ($mM^{-1}\ min^{-1}$)	% Efficiency
Xylitol	2000 ± 50	8.83 ± 1.02	227 ± 27	100
D-Sorbitol	1770 ± 70	21.8 ± 2.8	81.2 ± 11	36
Adonitol	1400 ± 60	30.5 ± 4.5	46.0 ± 7.0	20
D-Mannitol	380 ± 20	190 ± 28	2.00 ± 0.31	0.9
L-Arabitol	300 ± 20	298 ± 49	1.01 ± 0.18	0.4

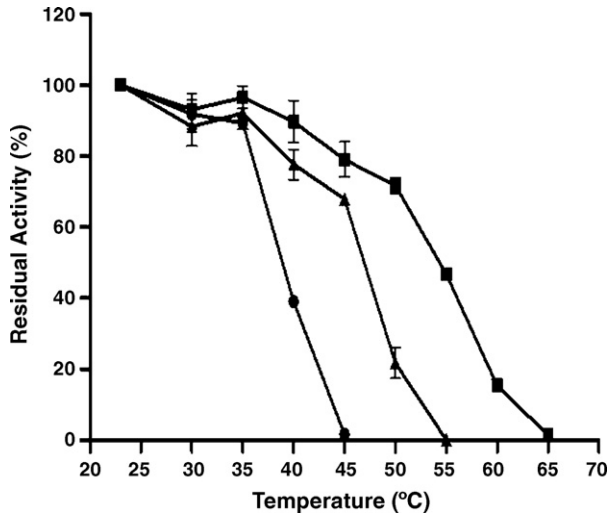

Fig. 3. Thermal inactivation of recombinant XDHs at various temperatures for 15 min: (●) wild-type caXDH, (▲) C4/ARSdR mutants, and (■) C4/ARS mutants.

so far for a reversal of the cofactor preference. In contrast to the engineered $NADP^+$-dependent psXDH, the mutants created in this research showed better catalytic efficiency and lower K_M towards $NADP^+$ (Table 2), which distinguished the mutated caXDH from that of *P. stipitis*.

Sequence alignment with the known medium chain XDHs revealed that wild-type XDH of *C. albicans* shared high identity with the known XDHs (Fig. 1), in which the highest identities are with *Candida tropicalis* and *P. stipitis* [16]. The amino acid residues corresponding to metal binding sites and cofactor-binding pockets were much conserved (Fig. 1). Not surprisingly, similar to the known XDHs from other microorganisms, the wild-type XDH from *C. albicans* is exclusively NAD^+-dependent. Interestingly, although XDH shared the highest identity with that from *C. tropicalis*, the catalytic efficiency of caXDH was 443-fold higher than wild-type ctXDH [16].

Similar to the known psXDH engineered for cofactor shifting, post site-directed mutagenesis, both mutants, C4/ARS and C4/ARSdR, have shifted the cofactor dependence. In contrast to the engineered $NADP^+$-dependent psXDH, both mutants of caXDH had 2-fold higher catalytic efficiency (Table 1) than those of mutants of psXDH with $NADP^+$ as a cofactor ($10{,}700 \pm 200$ and $10{,}500 \pm 100\ min^{-1}\ mM^{-1}$, respectively) [13]. Another added benefit of these mutants was that both mutants demonstrated better thermostablity than wild-type XDH since three additional cysteines were introduced into wild-type XDH for Zn^{2+} binding to stabilize the protein structure.

Surprisingly, when the purified recombinant XDHs were subjected to denaturing SDS-PAGE, a shift in electrophoretic mobility of mutants was observed. The recombinant C4ARS and C4ARSdR showed higher apparent molecular weight than that of wild-type. The introduction of those point mutations, however, does not account for the mass difference between mutants and wild-type XDH. We repeated the gel electrophoresis several times and obtained similar gel patterns as indicated in Fig. 2. We ruled out the presence of intra-molecular disulfide bonds in C4ARS and C4ARSdR mutants through the pretreatment of recombinant enzymes with 2-β-mercaptoethnol in the SDS sample buffer. Another possibility could be the presence of Zn^{2+} in functional XDHs which chelated cysteine residues introduced and thus affected the unfolding of the mutants under denaturing condition. Therefore, purified recombinant XDHs were treated with 0.5 M EDTA at pH 8.0 prior to electrophoresis. Unexpectedly, there was no difference in the electrophoretic behavior between EDTA-treated samples and samples without EDTA treatment (supplementary data). One possible explanation suggested by McLachlin and Dunn [20] to explain the abnormal electrophoretic mobility of mutant proteins containing the introduced cysteine point mutations was attributed to a conformational effect rather than an increase in molecular weight despite the presence of SDS. The shift of electrophoretic mobility could also be utilized to distinguish the mutant proteins containing the introduced cysteine point mutations from the wild-type protein on SDS-PAGE [20]. This is in accordance with our findings. Thus, we reasoned that the three more cysteine residues introduced in C4ARS and C4ARSdR altered the conformation of the wild-type XDH and led to the anomalous electrophoretic mobility of those two mutants.

It is generally accepted that due to cofactor imbalance and lower activity of XDH heterologously introduced, xylitol accumulation in recombinant *S. cerevisiae* bearing the xylose pathway from fungus is a major problem for efficient xylose utilization. As expected, the reconstructed *S. cerevisiae* bearing $NADP^+$-dependent psXDH and wild-type psXR indicated lower level xylitol accumulation compared to the construct having cofactor-imbalanced xylose pathway [14]. Since the engineered $NADP^+$-dependent XDH in this research has higher catalytic efficiency than its homolog, the $NADP^+$-dependent psXDH [13], it could be an alternative candidate for construction of a recombinant *S. cerevisiae* with a cofactor-balanced xylose pathway. Hence, we can expect the new constructs containing psXR and ca-C4/ARS to perform better than that bearing psXR and ps-C4/ARS gene cassettes.

5. Conclusions

The recombinant wild-type XDH from *C. albicans* is strictly NAD^+-dependent. Post site-directed mutagenesis, the cofactor dependence of XDH was shifted from NAD^+ to $NADP^+$. The engineered XDH with a shift of cofactor preference in this work will be a potential enzyme source for construction of a cofactor-balanced xylose utilization pathway in *S. cerevisiae* for bioethanol production.

Acknowledgements

We thank Kelvin Koh Jian Long and Yongkai Goh for their help in the purification of the recombinant proteins and Mrs. Lily Tan and Dr. Balaji Balagurunathan for helpful discussion. A*STAR of Singapore funded this project ICES/07-173B01.

Appendix A. Supplementary data

Supplementary data associated with this article can be found, in the online version, at doi:10.1016/j.molcatb.2009.08.013.

References

[1] M. Galbe, G. Zacchi, Appl. Microbiol. Biotechnol. 59 (2002) 618–628.
[2] T.W. Jeffries, Curr. Opin. Biotechnol. 17 (2006) 320–326.
[3] A.J.A. van Maris, A.A. Winkler, M. Kuyper, W.T.A.M. de Laat, J.P. van Dijken, J.T. Pronk, Adv. Biochem. Eng./Biotechnol. 108 (2007) 179–204.
[4] N.W. Ho, Z. Chen, A.P. Brainard, Appl. Environ. Microbiol. 64 (1998) 1852–1859.
[5] A. Eliasson, C. Christensson, C.F. Wahlbom, B. Hahn-Hägerdal, Appl. Environ. Microbiol. 66 (2000) 3381–3386.
[6] M. Kuyper, M.M. Hartog, M.J. Toirkens, M.J. Almering, A.A. Winkler, J.P. van Dijken, J.T. Pronk, FEMS Yeast Res. 5 (2005) 399–409.
[7] N. Meinander, I. Boels, B. Hahn-Hägerdal, Bioresour. Technol. 68 (1999) 79–87.
[8] B. Hahn-Hägerdal, C.F. Wahlborn, M. Gardonyi, W.H. van Zyl, R.R.C. Otero, L. Jonsson, Adv. Biochem. Eng./Biotechnol. 73 (2001) 53–84.
[9] T.W. Jeffries, N.Q. Shi, Adv. Biochem. Eng./Biotechnol. 65 (1999) 117–161.
[10] B. Hahn-Hägerdal, K. Karhumaa, C. Fonseca, I. Spencer-Martins, M. Gorwa-Grauslund, Appl. Microbiol. Biotechnol. 74 (2007) 937–953.
[11] A. Lönn, K.L. Träff-Bjerre, R.R.C. Otero, W.H. van Zyl, B. Hahn-Hägerdal, Enzyme Microbial Technol. 32 (2003) 567–573.
[12] M. Jeppsson, O. Bengtsson, K. Franke, H. Lee, B. Hahn-Hägerdal, M.F. Gorwa-Grauslund, Biotechnol. Bioeng. 93 (2006) 665–673.
[13] S. Watanabe, T. Kodaki, K. Makino, J. Biol. Chem. 280 (2005) 10340–10349.
[14] A. Matsushika, S. Watanabe, T. Kodaki, K. Makino, H. Inoue, K. Murakami, O. Takimura, S. Sawayama, Appl. Microbiol. Biotechnol. 81 (2008) 243–255.
[15] T. Jones, N.A. Federspielb, H. Chibana, J. Dungan, S.B.B. Kalman, G. Newport, Y.R. Thorstenson, N. Agabian, P.T. Magee, R.W. Davis, S. Scherer, Proc. Natl. Acad. Sci. U.S.A. 101 (2004) 7329–7334.
[16] B.S. Ko, H.C. Jung, J.H. Kim, Biotechnol. Prog. 22 (2006) 1708–1714.
[17] G. Panagiotou, D. Kekos, B.J. Macris, P. Christakopoulos, Biotechnol. Lett. 24 (2002) 2089–2092.
[18] L.H. Tran, N. Kitamoto, K. Kawai, K. Takamizawa, T. Suzuki, J. Biosci. Bioeng. 97 (2004) 419–422.
[19] E. Boer, T. Wartmann, S. Schmidt, R. Bode, G. Gellissen, G. Kunze, Antonie Van Leeuwenhoek 87 (2005) 233–243.
[20] D.T. McLachlin, S.D. Dunn, Pro. Exp. Purif. 7 (1996) 275–280.